Lateral Jet Control of a Supersonic Missile: Computational and Experimental Comparisons

B. Srivastava*
Raytheon Company, Tewksbury, Massachusetts 01876-0901

Several three-dimensional, viscous, turbulent Navier–Stokes computations have been performed for a missile equipped with and without divert jet thruster for three different wing planforms (having a fixed tail configuration) at a nominal flow Mach number of 3.94, angles of attack ranging from 2 to 25 deg, and jet thrust ratios of one and four. Results are presented to show that the normal force and pitching moment coefficients for all computed cases are predicted within 5% of the wind-tunnel data. Synthesis of all of the results show low amplification factor for all windward jet thruster cases. For this case the upstream favorable pressure zone created by the windward jet is insufficient to compensate for the massive unfavorable pressure loss on the windward wings/tails due to the jet blockage and jet wraparound effects.

Nomenclature

AF	=	amplification factor, $1 + (CN_{\text{jet}} - CN_{\text{no-jet}})/(T/q \cdot S)$
alpha	=	angle of attack, deg
CM	=	$F_N \cdot (X_{\text{mc}} - X_{\text{cp}})/(q \cdot S \cdot X_{\text{ref}})$
CN	=	normal force coefficient, $(N/q \cdot S)$
dp	=	pressure differential, $(P_{\text{jet}} - P_{\text{no-jet}})/(\text{gamma} \cdot P_{\text{inf}})$
gamma	=	ratio of specific heats
M	=	freestream Mach number
N	=	normal force, N
P	=	pressure, N/m^2
phi	=	azimuth angle, deg
q	=	dynamic pressure, $\frac{1}{2}\rho v^2$
S	=	missile cross-sectional area, m^2
T	=	jet thrust, N
v	=	velocity, m/s
X_{mc}	=	moment reference distance
X_{ref}	=	reference length (cylinder diameter)

Subscripts

inf	=	freestream condition
jet	=	condition with jet
no-jet	=	condition with no jet

Introduction

RAPID airframe response time is critical during the homing phase of interceptor missiles. Surface-mounted, fast-reacting jet thrusters offer an attractive alternative to conventional aerodynamic surface control for improved missile agility and maneuverability. Performance enhancements at low speed and high altitude (where dynamic pressure is low) are additional advantages of the surface reaction jets. It has been found that, under some missile orientations and flow conditions, the surface-mounted lateral jet leads to thrust amplification due to a high-surface-pressure region that forms ahead of the jet on the missile surface. Effective exploitation of the thrust amplification can lead to improved missile performance. However, it has also been observed that, at certain other flow conditions and orientations, the reaction jets can produce negative effects, i.e., thrust deamplification. An understanding of the controlling factors that produce high amplification as well as those

that produce low amplification is critical in developing a credible design basis for optimal missile performance.

The problem of the lateral jet interaction with the external flow under conditions of varying flight Mach numbers, angles of attack, and jet orientations is extremely complex in nature and has been studied experimentally and analytically for many years.[1,2] More recently, computational fluid dynamics (CFD) studies[3-7] have been performed to understand these effects. Our approach is to judiciously combine wind-tunnel testing and CFD simulation in an effort to evolve a validated design and analysis tool that can synthesize the physical complexity of the flow and identify its key controlling parameters. This paper deals with the overall CFD validations with and without lateral jet thrusters and subsequently outlines the utility of the approach for lateral jet effectiveness studies in relation to a missile design.

This paper is subdivided into several sections. The next section briefly outlines the previous work in this area using CFD approaches. The details of the computational methodology, geometry, grid-related issues, and boundary conditions for the CFD application are discussed later. CFD validation studies for a generic class of missile airframes with and without lateral thrusters are then compared with the wind-tunnel data for the normal forces and moments. The last section presents the overall summary and conclusions for the paper.

Background

The topic of jet interaction with an external supersonic flow dates back to the mid-1960s,[1,2] when a large number of generic experimental data were generated and related correlation techniques were developed. The emergence of hypersonic interceptors, the maturity of CFD, and the advent of supercomputers revived these activities in the late 1980s.[3-7] Several investigators have performed CFD studies for the fundamental problem of jet interaction in relation to adaptive gridding,[8] turbulence models,[9] grid refinements,[10] and the impact of artificial viscosity.[8] These studies range from Euler[11] to Navier–Stokes[12] computations. Of these studies, particular reference is made to the reported studies[6,12] because much of the current CFD effort is derived from their mature technical expertise in this area. Further details of the methodology and related research work can be obtained from the references cited.

Whereas a vast number of numerical studies have been performed using controlled jet interaction studies for methodology development, efforts to simulate missile surfaces have been rather limited. More recently, Chan et al.[13] performed a series of studies that lead to the simulation of a full missile surface with control surfaces and jet interaction. Qin and Foster[14] also performed similar studies using a Navier–Stokes approach for an inclined jet on an ogive/cylinder body. These results depict the remarkable flow details obtained using CFD approaches, which ultimately result in making judicious

*Senior Development Engineer, System Design Laboratory, Raytheon Electronic Systems. Senior Member AIAA.

choices for flight vehicle design and further wind-tunnel testing. Srivastava[15] performed full Navier–Stokes studies for generic missile bodies with/without leeward and windward jets but without wing or tail panels. Comparisons with the wind-tunnel data, however, was not direct because the tests were conducted with tail panels, whereas computations were performed without tail. Removal of the tail load from the wind-tunnel data by an approximate method introduced uncertainties that were not fully quantified. This deficiency in the CFD model has been eliminated in the current paper, which shows direct comparison of the CFD predictions with the wind-tunnel data by modeling all geometrical aspects of the wind-tunnel missile geometry.

Computational Methodology

PARCH,[6] which is a full Navier–Stokes (FNS) code with plume/ missile airframe steady-flow predictive capability, is being used for our current studies. PARCH code utilizes formulations based on the NASA Ames Research Center ARC aerodynamic code and the Arnold Engineering Development Center (AEDC) propulsive extension, PARC. This code is particularly suited for missile surfaces due to its grid patching capability, which is useful for treating embedded surfaces in a flowfield. Patching that is accomplished in mapped computational coordinates is automatically constructed from boundary inputs. Boundary conditions are applied along the outer computational boundaries and relevant embedded surfaces. The code utilizes diagonalized Beam–Warming numerics with matrix-split finite rate chemistry. Several versions of the K–E turbulence model that were specifically developed for jet interaction and propulsive studies are available in the code. We are using the capped low-Reynolds-number formulation[12] for the current simulations. Further details of the code capability can be found in Ref. 6.

Typical boundary approaches for the current application (supersonic flows) are specified supersonic freestream conditions at the inlet and outer boundaries. Extrapolation procedures are employed at the exit boundary. Surface conditions are appropriate to viscous flows with adiabatic wall condition.

The surface jet boundary condition is the specified jet nozzle supersonic exit conditions. The circular area of the jet in the wind-tunnel test is approximated by a square aperture in the CFD simulation.

Figure 1 shows a sketch of the wind-tunnel models recently tested by Raytheon in the McAir Polysonic Wind-Tunnel with three different wing planforms. The wing in Fig. 1a is the baseline configuration, which is 15.734 in. long, and its leading edge starts 12.134 in. from the missile nose. The jet thruster is located 14 in. from the nose. The jet area is a 0.1764-in.^{2} circular hole. The second configuration, shown in Fig. 1b, is a forward wing configuration whose length is the same but whose leading edge is moved forward to 10.301 in. from the missile nose. The third configuration is a short wing, with a length of 7.67 in. and with the leading edge starting at 10.301 in. For all configurations, tail panel geometry and axial jet location are the same. This missile is rolled in the tunnel to achieve windward and leeward jet orientations. CFD simulations utilize the rotation of inlet velocity vector to simulate leeward and windward jet orientations. These simulations were performed on three different grids corresponding to the three configurations. The axial distribution of the grid was the only component that was modified, keeping the total number of grids the same, i.e., $230 \times 51 \times 69$, axial, normal, and circumferential in that order. The grid patching procedure was used to apply the relevant boundary conditions on the surfaces. All angles of attack for a given configuration were simulated on a single grid consistent with the minimum desired Mach number and maximum desired angle of attack. This allows us to minimize the grid effort. The grids were generated through GRIDGEN, with geometry models developed within GRIDGEN.[16]

The jet area was resolved by using a 10×10 grid on the missile surface. The boundary conditions on this jet area grid were specified by inputting the exit conditions of a nozzle analysis using an iterative procedure consisting of the nozzle exit area, isentropic conditions, and specified jet thrust. Local time stepping procedures with conventional dissipation factors were employed to achieve convergence defined by at least three orders of magnitude reduction in the maximum residual. Converged solutions were checked with three and four orders of magnitude reduction in the maximum residual for selected cases. The minimum grid spacing near the missile surface was assigned by choosing a y^+ value of 5 for all computations. Variation of this value did not produce any significant changes in the predicted results. Postanalysis of the computed cases later suggested that the external flow is primarily supersonic and the vortical flow nature around the missile geometry is primarily governed by the inviscid phenomena. Selected test cases with inviscid CFD simulations showed that force and moment coefficients can be well predicted using inviscid models.

Comparison with Wind-Tunnel Tests

Our effort was confined to a nominal flow Mach number of 3.94 with angles of attack varying from 2 to 25 deg. Exact wind-tunnel conditions were used for each CFD simulation. CFD efforts were restricted to leeward and windward jet orientations, which encompass the most severe flow cases. This also allows us to exploit symmetry in CFD simulation. Jet thrusts were simulated at the wind-tunnel test conditions of 175 and 50 lb (nominal cases).

Baseline Wings
Windward Jets

Figure 2 shows the computed surface pressure contours for two cases. At top is a windward jet, jet thrust of 175 lb, flow Mach number of 3.94, and angle of attack of 20 deg. For this case, notice the extent of high pressure forward of the jet and very low pressures aft of the jet on the windward side. It is quite clear that in the presence of the jet-on condition the jet has totally wiped out the aft normal forces created by the windward wings. This is clearer if we compare the lower figure, which shows jet-off pressure contours, with the jet-on upper figure. The table inset in Fig. 2 shows the comparison of the normal force and pitching moment coefficients with the wind-tunnel data. The comparisons are excellent. Overall the following can be concluded from Fig. 2.

1) A windward-located jet thruster creates a favorable high-pressure zone ahead of the jet but only at the expense of a massive loss of normal force from the windward wings.

2) For this case the thrust amplification factor [defined as (1 + aero-interactive force/thrust), where aero-interactive force is equal to jet-on normal force on the airframe minus jet-off normal force on the airframe] is 0.56. Note, however, that the pitching moment is significantly increased with the jet thrusters. Even though the latter can be used effectively to our advantage for vehicle maneuver, our goal is to also enhance the force amplification factor.
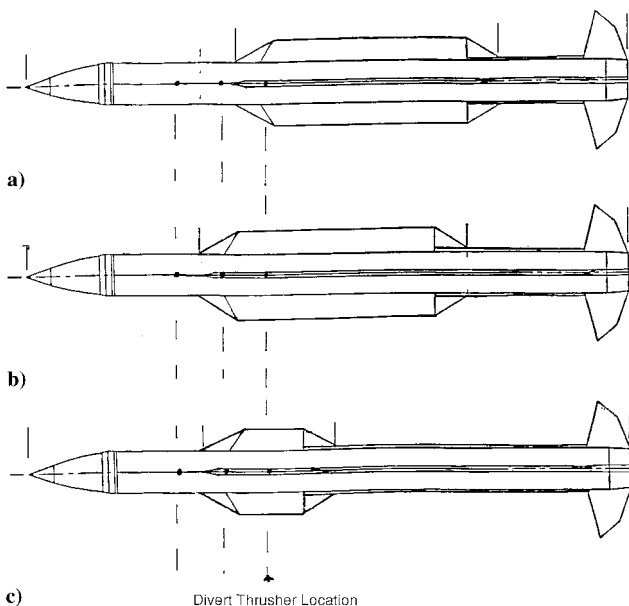

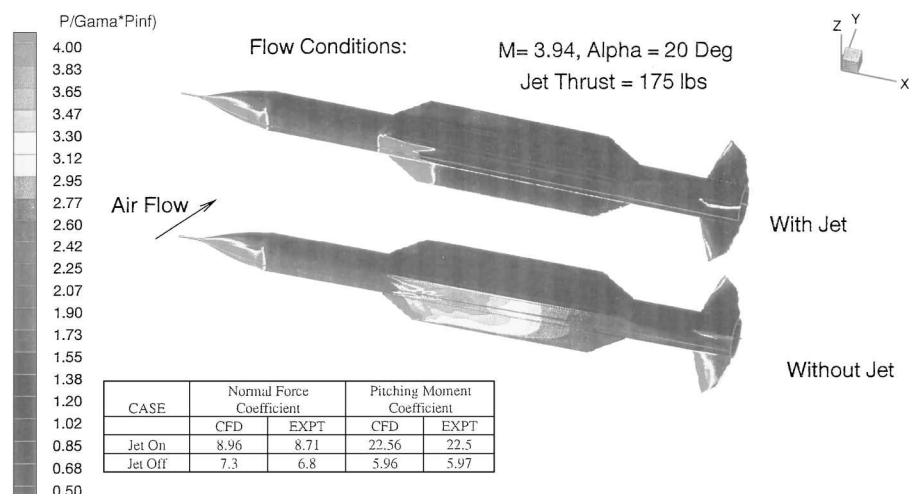**Fig. 1 Wind-tunnel test geometry for a generic missile.**

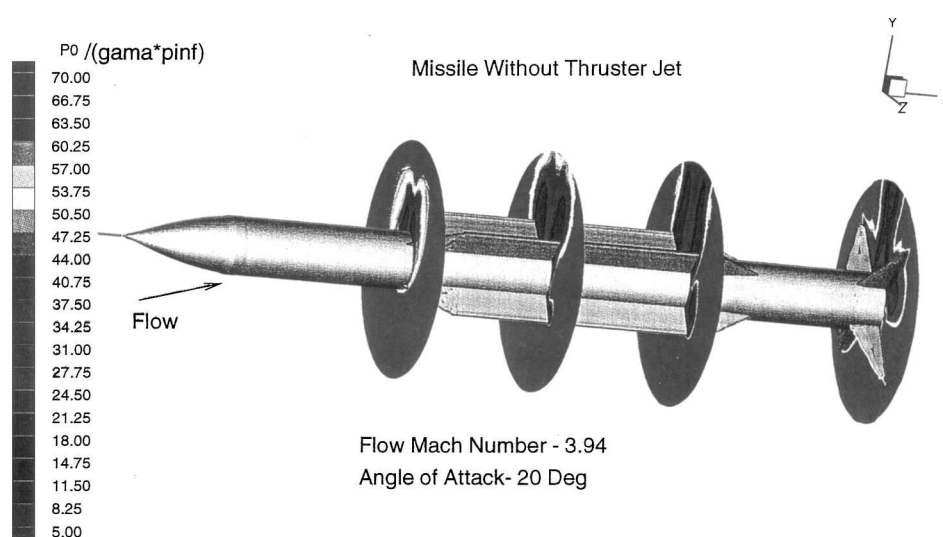**Fig. 2   Pressure distribution for the wind-tunnel missile geometry with and without windward jet.**

Fig. 3   Total pressure contours at several axial locations showing vortex formation without jet.

3) Note also from Fig. 2 that a jet wraparound effect is seen to create an adverse effect causing undesirable normal forces.

4) The effect of the jet gas on the tail panels is also massive, resulting in the loss of tail control power for this jet orientation.

These effects were observed in our previous computations,[15] but now the results are far more credible due to the excellent comparisons with the wind-tunnel data. The vortical flow pattern of the missile with and without the windward jet can be observed from Fig. 3, where the total pressure contours for several axial locations of the missile without the divert thruster are shown. Note that the early formation of the body vortices on the leeward side forward of the wings, which interact with the leeward wings, are subsequently modified and later interact with the tail panels. Additional vortices are generated on the leeward side of the lower wings that later follow an upward path, as seen in Fig. 3. For these flow conditions, the inviscid effects dictate the vortical flow structure.

Figure 4 shows a similar plot with a windward divert thruster. Note that the jet effects result in massive loss of the total pressure, first on the windward side but gradually wrapping around the missile downstream to engulf the leeward side of the missile surfaces.

Similar computations for a lower jet thrust of 50 lb at identical flow conditions yield excellent comparison with the wind-tunnel data (Table 1). For this case the thrust amplification factor is −0.17, indicating that the thruster loses its effectiveness except for the gains in the moment coefficient. Figure 5 shows the results in a different format. In an effort to enhance the interactive effects, a pressure differential plot between the jet-on and jet-off cases is shown for high- and low-thrust cases. Note from Fig. 5 that the high-pressure zone ahead of the jet, wraparound effects of the jet, and massive

loss of pressure forces on windward wing and tail panels are the controlling physical mechanisms.

At a jet thrust of 175 lb, the comparisons for other angles of attack are shown in Table 1. Note that, at an angle of attack of 10.8 deg, comparisons with the wind-tunnel experiment remain excellent, as they do for an angle of attack of 4.02 deg.

Further computations were made for angles of attack of 9.95 and 3.13 deg without the jet thrusters to validate the CFD results at low angles of attack. These results are shown in Table 1. Predicted results are in excellent comparison with the experimental data.

Leeward Jets

Further CFD computations for validation were performed for leeward jet orientation. Two thrust levels were computed, 175 and 50 lb. The angle-of-attack range was from 2.2 to 20 deg at a nominal flow Mach number of 3.94. All of the computed results are excellent in comparison with the wind-tunnel data (Table 1). Figure 6 shows two views of the computed results for a jet thrust of 175 lb at an angle of attack of 19 deg. View I shows the leeward side, whereas view II shows the windward side. A comparison of Fig. 6 with Fig. 2 indicates the following.

1) For a leeward jet thruster, there is only a marginal positive pressure gain ahead of the jet because the jet exhausts in a vortical flow zone.

2) The windward wings and missile body pressure levels are also affected, as is seen if we compare Fig. 6 view II with the jet-off windward side in Fig. 2.

3) Comparison with the experimental data is excellent.

Figure 7 shows the vortical flow pattern for the leeward divert thruster. Note from the total pressure contours of Fig. 7 that the

Table 1   Comparisons of CFD and wind-tunnel (Exp.) force and moment coefficients

Case no.	Mach number	Angle of attack, deg	Jet thrust T, lb	CN CFD	CN Exp.	CM CFD	CM Exp.
1, BW[a]	3.94	20	175	8.96	8.71	22.56	22.5
2, BW[a]	3.94	20	0	7.3	6.8	5.96	5.97
3, BW[a]	3.94	20	50	6.91	6.63	11.96	12.28
4, BW[a]	3.94	10.8	175	6.54	6.30	16.03	15.76
5, BW[a]	3.94	4.02	175	4.86	4.70	13.48	13.26
6, BW[a]	3.94	9.95	0	2.83	2.84	2.71	2.89
7, BW[a]	3.94	3.13	0	0.73	0.79	0.91	1.081
8, BW[a]	3.94	19.0	−175	2.49	2.35	−6.09	−6.20
9, BW[a]	3.94	20.0	−50	5.55	5.46	2.15	2.24
10, BW[a]	3.94	9	−175	−1.47	−1.4	−9.4	−9.09
11, BW[a]	3.94	2.2	−175	−3.39	−3.3	−11.59	−11.37
12, FW[b]	3.94	25.0	175	11.13	10.77	29.24	29.70
13, FW[b]	3.94	25.0	0	9.28	9.17	11.03	11.66
14, FW[b]	3.94	25.0	102	9.66	9.40	23.03	23.52
15, SW[c]	3.94	20.0	175	9.31	8.97	25.11	25.32
16, SW[c]	3.94	20.0	50	6.45	6.02	13.78	13.68
17, SW[c]	3.94	20.0	0	5.53	5.15	7.65	7.49

[a]Baseline wing.   [b]Forward wing.   [c]Short wing.
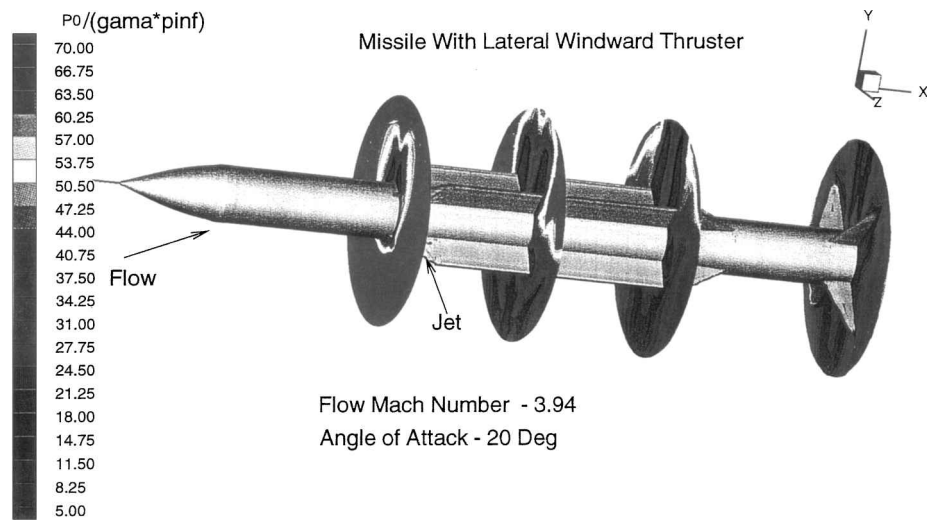
Fig. 4   Total pressure contours at several axial locations showing windward jet effects.
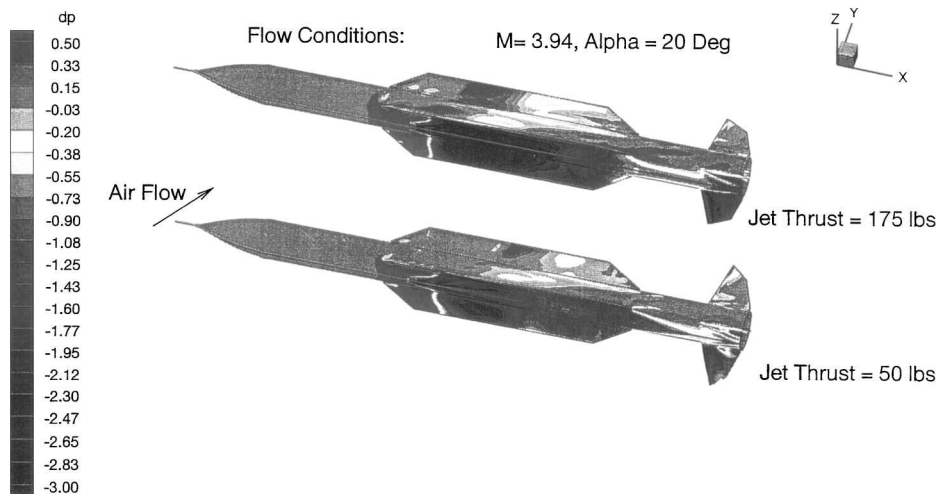
Fig. 5   Missile surface pressure differential for jet-on and jet-off cases showing jet wraparound high-pressure effects.

effect of the leeward jet is confined between the two leeward wings. This indicates that, for leeward jets, jet effects are confined to the leeward side of the missile surfaces.

Similar comparison for a leeward jet with a jet thrust of 50 lb and an angle of attack of 20 deg is shown in Table 1. The comparison of the computed results with the experimental data is excellent. Other comparisons at lower angles of attack of 9 and 2.2 deg are shown in Table 1.

Forward Wings

In an attempt to understand the effects of the jet thruster location in relation to the missile wings, tests were conducted with wings moved forward of the jet location by 1.83 in. The objective was to attempt to enhance the positive pressure effects forward of the jets, for windward jet orientation, in an effort to enhance amplification factors. Figure 8 shows the computations with a forward wing, with and without windward jets, at an angle of attack of 25 deg and a
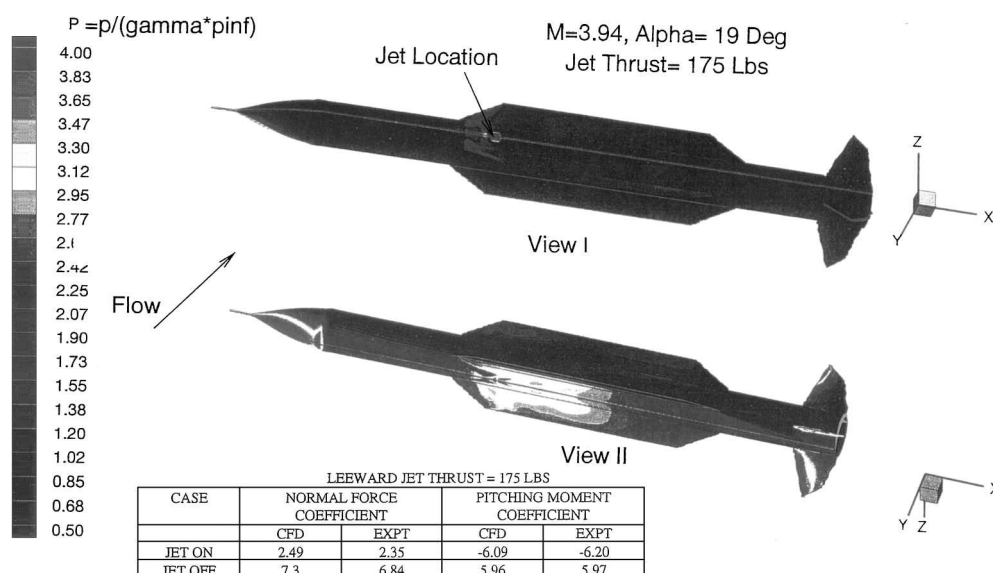
CASE	NORMAL FORCE COEFFICIENT		PITCHING MOMENT COEFFICIENT	
	CFD	EXPT	CFD	EXPT
JET ON	2.49	2.35	-6.09	-6.20
JET OFF	7.3	6.84	5.96	5.97

Fig. 6   Pressure distribution on missile surfaces showing leeward jet interaction effects.
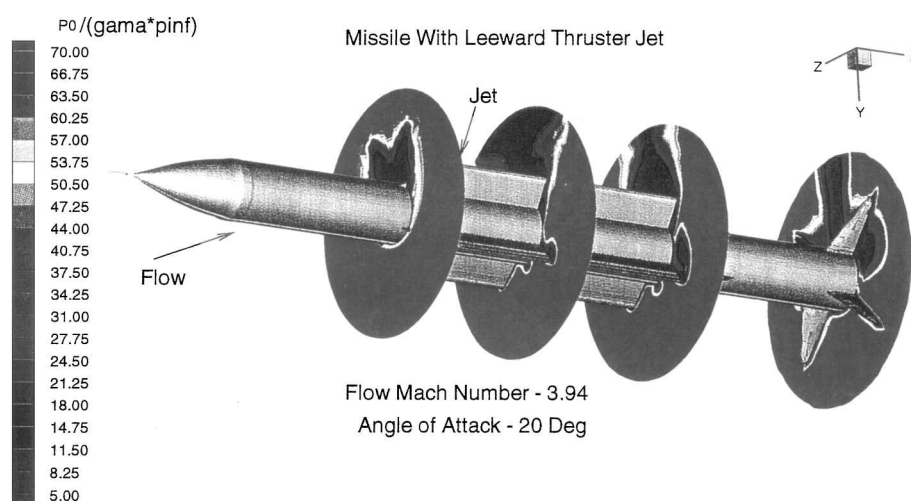

Fig. 7   Total pressure contours at several axial locations showing leeward jet interaction effects.

nominal flow Mach number of 3.94. Once again, the comparisons between the computed results and wind-tunnel data are good, as seen from the table inset in Fig. 8. It is also observed that, with a forward wing, the positive pressure zone is somewhat larger than that in Fig. 2 for the baseline wing. (Note that the angle of attack is lower in Fig. 2.) The amplification factor for this case is 0.47. This happens because the loss of positive pressure on the windward wings due to the jets effects still dominates the gain ahead of the jet. This phenomenon also persists at a lower jet thrust level of 102 lb (see Table 1).

Short Wings

A short wing (length 7.672 in. as compared to the baseline case of 15.734 in.) missile was also tested in the wind tunnel to investigate jet effects. Figure 9 shows the computed results for this case at an angle of attack of 20 deg and a flow Mach number of 3.94, with and without jet effects. The overall CFD comparisons for normal and pitching moment coefficients are still excellent, as shown in the table inset in Fig. 9. The amplification factor for this case is 1.12, which compares to 0.56 for the baseline wing at the same condition. It would appear, at least superficially, that significant gains in amplification factor may be achieved by careful selection of wing planform and the location of the lateral jet relative to the wing. The same behavior was observed at a reduced jet thrust level of 50 lb. As before, the pressure differential between the jet-on and the jet-off conditions highlights the jet wraparound effect

and loss of tail load with the jet-on conditions (see Ref. 17 for details).

Rolled Baseline Wings

When the missile is rolled such that one of the wings is vertically downward, the vortical flow pattern is likely to be influenced. The computational results and comparison with experiments for this missile orientation are discussed next.

Figure 10 shows the computed pressure contours for this orientation of the missile at an angle of attack of 20 deg and a flow Mach number of 3.94. Figure 10 also shows that comparison of the experimental data with the computed force and moment coefficients is excellent.

Note that the experiments were at a slightly different condition that introduces asymmetry, whereas CFD computations were made for a symmetric case. Note that the horizontal wings are highly loaded for this orientation of the missile.

Overall Results

All of the predicted results from CFD and wind-tunnel tests for the normal force coefficients and the pitching moment coefficients are shown in Figs. 11 and 12, respectively, indicating the degree of deviation of the predicted results from the wind-tunnel data. Note that both curves show very little deviation from the desired 45-deg line. The corresponding data are shown in Table 1.
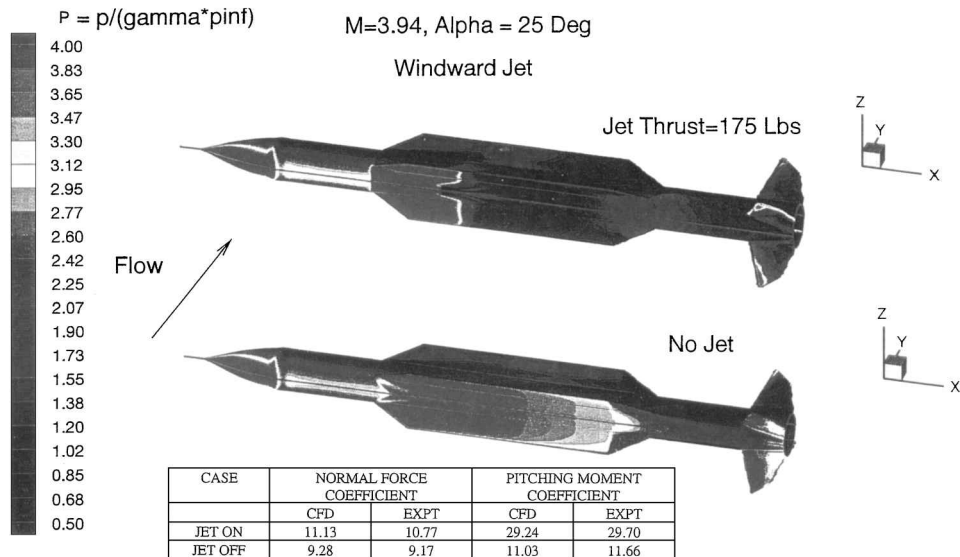
P = p/(gamma*pinf)   M=3.94, Alpha = 25 Deg

Windward Jet

Jet Thrust=175 Lbs

Flow

No Jet

CASE	NORMAL FORCE COEFFICIENT		PITCHING MOMENT COEFFICIENT	
	CFD	EXPT	CFD	EXPT
JET ON	11.13	10.77	29.24	29.70
JET OFF	9.28	9.17	11.03	11.66

Fig. 8   Pressure distribution on missile surfaces for forward wing configuration with and without windward jet.

P =(p/gamma*pinf)   M= 3.94, Alpha= 20 Deg

Jet Thrust= 175 Lbs

Flow

No Jet

CASE	NORMAL FORCE COEFFICIENT		PITCHING MOMENT COEFFICIENT	
	CFD	EXPT	CFD	EXPT
JET ON	9.31	8.97	25.11	25.32
JET OFF	5.53	5.15	7.65	7.49
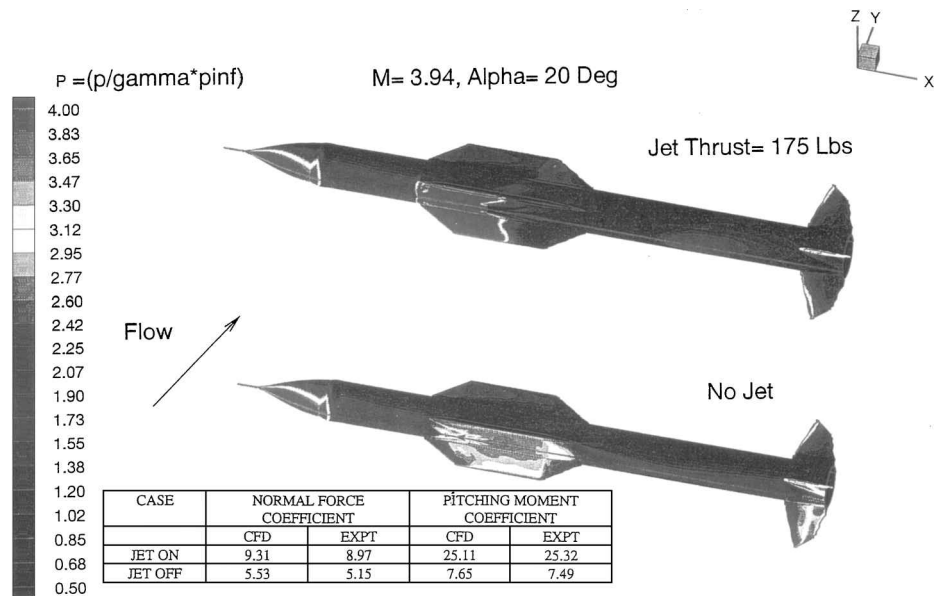
Fig. 9   Pressure distribution on missile surfaces for short wing configuration with and without windward jet.

P /(gama*pinf)

Flow Mach Number - 3.94
Angle of Attack - 20 Deg

Flow

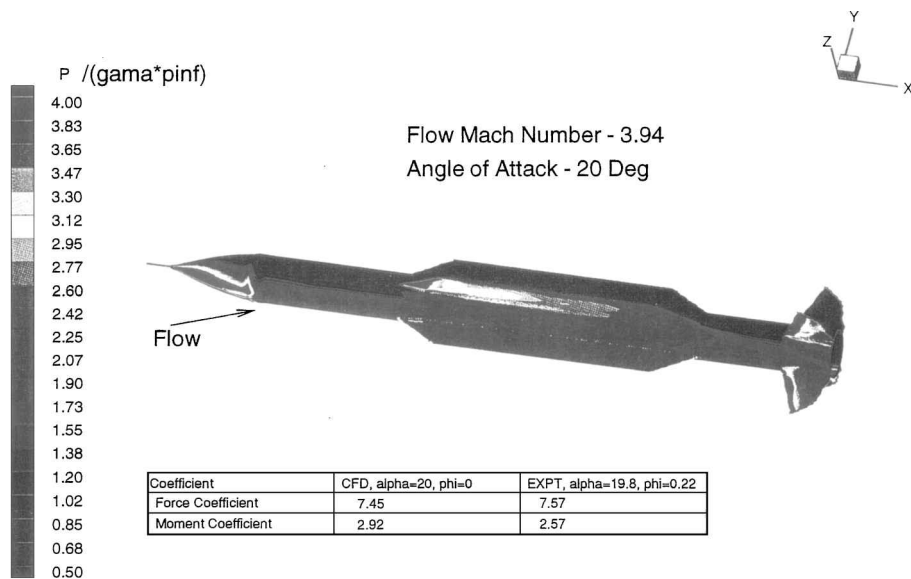| Coefficient	CFD, alpha=20, phi=0	EXPT, alpha=19.8, phi=0.22
Force Coefficient	7.45	7.57
Moment Coefficient	2.92	2.57

Fig. 10   Missile surface pressure distribution for a plus orientation without jet.
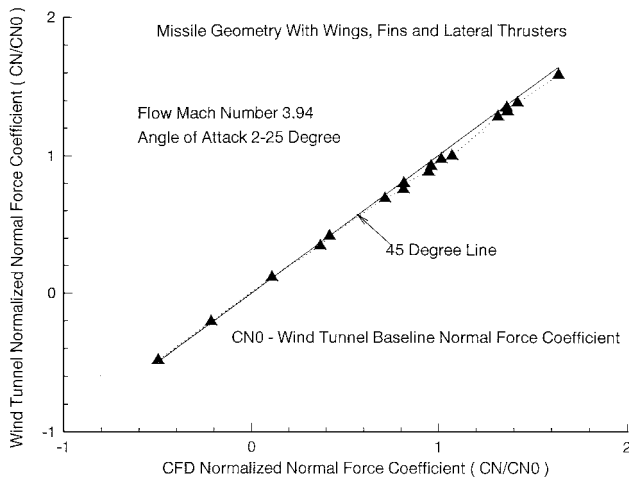
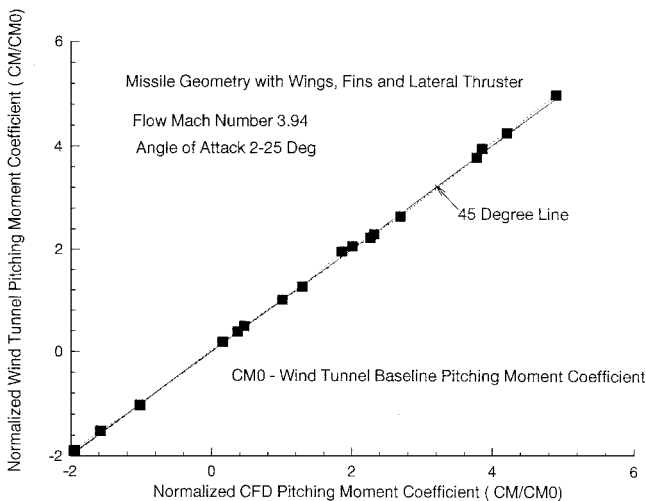**Fig. 11   Comparison of CFD and wind-tunnel normalized normal force coefficient.**

Fig. 12   Comparison of CFD and wind-tunnel normalized pitching moment coefficient.

Conclusions

Using CFD, 18 widely varying wind-tunnel test cases, encompassing geometry variations (baseline, forward, and short wings), angles of attack (2–25 deg), lateral jet-on with windward and leeward orientations and jet-off, were simulated to show that the normal force and moment coefficients for all cases are in excellent agreement with the data. Figure 11 for the normal force coefficient and Fig. 12 for the pitching moment coefficient sum up the overall accuracy of the predicted results for all of the cases considered. These validations demonstrate that our current CFD methodology can provide accurate predictions of the force and moment coefficients at widely varying flow conditions. Additionally, synthesis of the CFD results for various cases highlight the physical

mechanisms that inhibit the jet amplification factor for windward jet orientation.

References

[1] Cassel, L. A., Davis, J. G., and Engh, D. P., "Lateral Jet Control Effectiveness Prediction for Axisymmetric Missile Configurations," U.S. Army Missile Command, Rept. RD-TR-68-5, Redstone Arsenal, AL, June 1968.

[2] Spring, D., "An Experimental Investigation of the Interference Effects due to a Lateral Jet Issuing from a Body of Revolution over the Mach No. Range of 0.8 to 4.5," U.S. Army Missile Command, Rept. RD-TR-68-10, Redstone Arsenal, AL, Aug. 1968.

[3] Chamberlain, R., "Control Jet Interaction Flowfield Analysis," Lockheed Rept. LMSC F268936, *Aerodynamic Investigations*, Vol. 5, Feb. 1990.

[4] Chamberlain, R., "Calculation of Three-Dimensional Jet-Interaction Flowfields," AIAA Paper 90-2099, July 1990.

[5] Weatherly, D., and McDonough, J., "Performance Comparisons of Navier–Stokes Codes for Simulating Three-Dimensional Hypersonic Cross-flow/Jet Interaction," AIAA Paper 91-2096, June 1991.

[6] York, B. J., Sinha, N., Kenzakowski, D. C., and Dash, S. M., "PARCH Code Simulation of Tactical Missile Plume/Airframe/Launch Interactions," *19th JANNAF Exhaust Plume Technology Meeting*, CPIA PWB 568, Chemical Propulsion Information Agency, Laurel, MD, 1991, pp. 645–674.

[7] Chan, S. C., and Roger, R. P., Edwards, G. L., and Brooks, W. B., "Integrated Jet Interactions CFD Predictions and Comparison to Force and Moment Measurements for a Thruster Attitude Controlled Supersonic Missile," AIAA Paper 93-3522, Aug. 1993.

[8] Lytle, J. K., Harloff, G. J., and Hsu, A. T., "Three-Dimensional Compressible Jet-in-Crossflow Calculations Using Improved Viscosity Models and Adapted Grid," AIAA Paper 90-2100, July 1990.

[9] Dash, S. M., Sinha, N., York, B. J., Lee, R. A., and Hosangadi, A., "On the Inclusion of Advanced Turbulence Models and Nonequilibrium Thermochemistry into State-of-the-Art CFD Codes and Their Validation," AIAA Paper 92-2764, May 1992.

[10] Rizzetta, D. P., "Numerical Simulation of Slot Injection into a Turbulent Supersonic Stream," AIAA Paper 92-0827, Jan. 1992.

[11] Darmieux, M., and Marasaa-Poey, R., "Numerical Assessment of Aerodynamic Interactions on Missiles with Transverse Jets Control," AGARD Meeting on Computational and Experimental Assessment of Jets in Cross Flow, April 1993.

[12] Dash, S. M., York, B. J., Sinha, N., Lee, R. A., Hosangadi, A., and Kenzakowski, D. C., "Recent Developments in the Simulation of Steady and Transient Transverse Jet Interactions for Missile, Rotorcraft, and Propulsive Applications," AGARD Meeting on Computational and Experimental Assessment of Jets in Cross Flow, April 1993.

[13] Chan, S. C., Roger, R. P., Brooks, W. B., Edwards, G. L., and Boukather, S. B., "CFD Predictions and Comparisons to Wind Tunnel Data for the Asymmetric Firing of a Forward Mounted Attitude Control Thruster," AIAA Paper 95-1895, June 1995.

[14] Qin, N., and Foster, G. W., "Study of Flow Interactions due to a Supersonic Lateral Jet Using High Resolution Navier–Stokes Solutions," AIAA Paper 94-2151, June 1994.

[15] Srivastava, B., "CFD Analysis and Validation for Lateral Jet Control of a Missile," AIAA Paper 96-0288, Jan. 1996.

[16] Steinbrenner, J. P., and Chawner, J. R., "Recent Enhancements to the GRIDGEN Structural Grid Generation System," *Proceedings of the NASA Workshop on Software Systems for Surface Modeling and Grid Generation*, Hampton, VA, 1992.

[17] Srivastava, B. N., "Lateral Jet Control of a Supersonic Missile: CFD Predictions and Comparison to Force and Moment Measurements," AIAA Paper 97-0639, Jan. 1997.

R. M. Cummings
Associate Editor